

that all of the compounds **2**, **4**, **6**, **9**, and **10** are *cis*- $\beta$  complexes.

Compounds **1**, **3**, **5**, **7**, and **9** were prepared under conditions previously shown to yield  $\alpha$ -dinitro and carbonato complexes, respectively, for the (trien)Co<sup>III</sup> moiety.<sup>6</sup> The vicinal effects observed for these compounds are quite similar to each other in character, with maxima near 365 and 450 nm and minima near 334, 400, and 530 nm (Figure 2-6). They exhibit distinctly different character from the vicinal effects of the  $\beta$  complexes and vary in maximum intensity from 12 to 30% of that of the isomeric *cis*- $\beta$  complexes. We therefore conclude that the compounds **1**, **3**, **5**, **7**, and **9** are all *cis*- $\alpha$  complexes.

It is evident that the *cis*- $\beta$  configuration is more stable than the *cis*- $\alpha$  in 3 M tartaric acid. Thus a solution of a  $\beta$ -dinitro complex held at 80 °C for several days maintains nearly the same character of the CD spectrum, which only gradually decreases in intensity as the solution fades and the complex undergoes slow decomposition, whereas the vicinal effect of a solution of the  $\alpha$  complex **3** begins to increase in magnitude and acquire characteristics of the corresponding  $\beta$  complex (Table I). Calculation using data from Table I and data abstracted from the curves in Figure 3 leads to the estimate that the undecomposed complex, after 4.75 days, is approximately an equal mixture of  $\alpha$  and  $\beta$  species. However, this time study reveals that the  $\alpha$ - $\beta$  isomerization is not sufficiently rapid to cause confusion in the results obtained over a 2-h heating period.

Just as it is not to be expected that the  $\Delta$  and  $\Lambda$  isomers of the racemic (trien)Co<sup>III</sup> complexes **1**, **2**, **7**, and **8** should react

with *d*-tartaric acid at equal rates, so it should not be expected that the optically active Co(III) complexes **3**, **4**, **5**, **6**, **9**, and **10** react equally rapidly with *d*- and *l*-tartaric acids. Because of this, the various diastereomers used to obtain the vicinal effects of Figures 2-6 may be at various degrees of completion in their reaction with tartaric acid at the end of 2 h. Thus these curves may not represent exact vicinal effects. It may also be that the vicinal effect curves are representative of a number of solution species and that determination of a proper vicinal effect must await isolation of a pure complex. However, these reservations do not detract from the efficacy of the method.

### Conclusion

Additivity of d-d CD spectra, as manifested through the distinctness of the vicinal effects (which may be ascribed to differences in the achiral chromophore between the *cis*- $\alpha$  and *cis*- $\beta$  complexes), has proven to be a remarkably facile technique for clearly discriminating between  $\alpha$  and  $\beta$  complexes of substituted (triethylenetetramine)cobalt(III) with carbonato and nitro ligands.

**Acknowledgment.** We gratefully acknowledge the support of the Colorado State University Experiment Station and of the Research Corp.

**Registry No.** **1**, 14873-88-2; **2**, 41593-00-4; **3**, 36537-99-2; **4**, 36800-14-3; **5**, 52138-28-0; **6**, 74112-73-5; **7**, 36994-86-2; **8**, 74081-98-4; **9**, 74082-00-1; **10**, 74112-75-7.

Contribution from the Departments of Chemistry, University of Houston, Houston, Texas 77004, and William Marsh Rice University, Houston, Texas 77001

## Spin State Dependent Redox Properties of the [Fe<sup>III</sup>(X-Sal)<sub>2</sub>trien]<sup>+</sup> Spin-Equilibrium System in Solution

KARL M. KADISH,<sup>\*1,2</sup> K. DAS,<sup>1</sup> D. SCHAEFER,<sup>1</sup> CONNIE L. MERRILL,<sup>3</sup> BYRON R. WELCH,<sup>3</sup> and LON J. WILSON<sup>3</sup>

Received December 7, 1979

The electroreduction of a series of iron(III) chelates having hexadentate Schiff base ligands, [(X-sal)<sub>2</sub>trien]<sup>2-</sup>, derived from triethylenetetramine (trien) and various substituted salicylaldehydes (X = H, NO<sub>2</sub>, OCH<sub>3</sub>, Br, Cl) has been investigated in nonaqueous media. The electron-transfer properties of the complexes are of special interest since the compounds are known to be <sup>2</sup>T = <sup>6</sup>A spin-equilibrium species in both the solid and solution states. In solution, the spin equilibria are dependent on solvent, on the X substituent, and, of course, on temperature. The reduction of the Fe<sup>III</sup>[(X-sal)<sub>2</sub>trien]<sup>+</sup> complexes involves a reversible, one-electron transfer. Half-wave potentials for the reductions were also found to be dependent on the substituent, nature of the solvent, and temperature. From the temperature dependence (220-300 K) of the half-wave potentials, (dE/dT)<sub>p</sub>, the electron-transfer entropy change for the reduction processes has been determined and a comparison made between the electron-transfer entropy and the entropy change associated with the spin equilibrium. A mechanism relating the spin equilibrium and the electroreduction is also proposed.

### Introduction

In recent years a number of electrochemical studies involving macrocyclic complexes as models for biological heme electron-transfer reactions have been published.<sup>4-6</sup> These electron-transfer reactions have been characterized with respect

to solvent media, coordination number, spin state, and position of the iron atom relative to the donor atom plane of the macrocyclic ligands. Although many relationships have been investigated, detailed information as to how changes in spin state affect the Fe(III)/Fe(II) electron-transfer reaction has not been reported.

Several papers have now been published which characterize spin equilibria in solution for various six-coordinate Fe(III)<sup>7-13</sup>

(1) University of Houston.

(2) To whom correspondence should be addressed.

(3) William Marsh Rice University.

(4) (a) K. Smith, Ed., "Porphyrins and Metalloporphyrins", Elsevier, New York, 1975; (b) D. T. Sawyer, Ed., *ACS Symp. Ser.*, No. 38 (1977).

(5) A. W. Addison, W. R. Cullen, D. Dolphin, and B. R. James, Eds., "Biological Aspects in Inorganic Chemistry", Wiley, New York, 1977.

(6) Dave Dolphin, Ed., "The Porphyrins", Vols. I-IV, Academic Press, New York, 1978.

(7) M. F. Tweedle and L. J. Wilson, *J. Am. Chem. Soc.*, **98**, 4824 (1976).

(8) E. V. Dose, K. M. M. Murphy, and L. J. Wilson, *Inorg. Chem.*, **15**, 2622 (1976).

(9) E. V. Dose, M. F. Tweedle, L. J. Wilson, and N. Sutin, *J. Am. Chem. Soc.*, **99**, 3886 (1977).

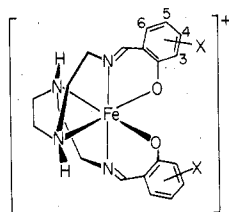
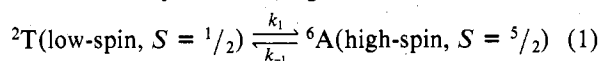


Figure 1. Structure of the  ${}^2T \rightleftharpoons {}^6A$  variable-spin [Fe(X-Sal)<sub>2</sub>trien]<sup>+</sup> cations.

and Fe(II)<sup>14-19</sup> complexes. These studies are of interest not only in terms of inorganic systems but also in terms of understanding biological electron-transfer reactions of those Fe(III) and Fe(II) metalloproteins in which spin equilibria may be involved.<sup>20-22</sup> Recently, the effect of a spin equilibrium on the oxidation-reduction potentials for tris(*N,N*-disubstituted-dithiocarbamato)iron(III) complexes has appeared.<sup>10,23,24</sup> Each of these complexes undergoes a  ${}^2T \rightleftharpoons {}^6A$  Fe(III) spin crossover, and each can be oxidized to an Fe(IV) complex. In this paper we wish to report the effect of the Fe(III) spin state on the reversible Fe(III)/Fe(II) reduction potentials for  ${}^2T \rightleftharpoons {}^6A$  spin-equilibrium complexes of hexadentate ligands derived from triethylenetetramine (trien) and various X-substituted salicylaldehydes (X-Sal), [Fe<sup>III</sup>(X-Sal)<sub>2</sub>trien]PF<sub>6</sub>.<sup>7</sup>

The [Fe<sup>III</sup>(X-Sal)<sub>2</sub>trien]<sup>+</sup> cations, whose general structure is shown in Figure 1, have been crystallographically structured<sup>25</sup> and shown to exhibit  ${}^2T \rightleftharpoons {}^6A$  spin equilibria in both solution and solid state.<sup>7,25</sup> In solution, the population of the high- and low-spin states for the compounds depend upon temperature, solvent, and the nature of the substituent, X. The dynamics of intersystem crossing for the



spin crossover has been obtained by laser-Raman *T*-jump<sup>12</sup> and ultrasonic relaxation<sup>13</sup> kinetics, with the first-order rate constants for the forward (*k*<sub>1</sub>) and reverse (*k*<sub>-1</sub>) reactions being in the range 10<sup>7</sup>-10<sup>8</sup> s<sup>-1</sup>. Since the spin-equilibrium phenomenon has direct relevance to some biological electron-transfer processes, we have undertaken a detailed electrochemical study of the [Fe<sup>III</sup>(X-Sal)<sub>2</sub>trien]<sup>+</sup> system to determine how the redox properties of this series of compounds depend on the equilibrium position of the thermally populated  ${}^2T$  and  ${}^6A$  spin states. Included in the study is the first reported variable-temperature

electrochemical investigation of the spin-equilibrium phenomenon in solution. In addition, the iron(II) compound, [Fe<sup>II</sup>(5-NO<sub>2</sub>-Sal)<sub>2</sub>trien], has been prepared, isolated, and characterized in order to identify the spin state of all the iron(II) reduction products.

### Experimental Section

**Materials and Syntheses.** Dichloromethane (CH<sub>2</sub>Cl<sub>2</sub>), acetone, dimethylformamide (DMF), nitromethane (CH<sub>3</sub>NO<sub>2</sub>), acetonitrile (CH<sub>3</sub>CN), butyronitrile (*n*-PrCN), dimethyl sulfoxide (Me<sub>2</sub>SO), and pyridine (py) were reagent grade; CH<sub>2</sub>Cl<sub>2</sub> was distilled from P<sub>2</sub>O<sub>5</sub>, and *n*-PrCN was stored over molecular sieves. For the electrochemistry, each solvent was made 0.1 M with tetrabutylammonium perchlorate (TBAP) as the supporting electrolyte. The TBAP was recrystallized from EtOH and dried under reduced pressure.

[Fe<sup>III</sup>(X-Sal)<sub>2</sub>trien]PF<sub>6</sub>. The iron(III) complexes were prepared as described earlier.<sup>7</sup>

[Fe<sup>II</sup>(5-NO<sub>2</sub>-Sal)<sub>2</sub>trien]. The 5-nitro iron(II) complex was prepared under N<sub>2</sub> from the iron(III) complex by controlled potential electrolysis (-0.50 V vs. SCE) in CH<sub>3</sub>CN (0.02 M in TBAP). Typically, a 100-mL solution, 3 × 10<sup>-3</sup> M in iron(III) complex (0.20 g), was electrochemically reduced for 30-40 min, during which time some of the iron(II) complex precipitated from solution as an iridescent gray-green solid. The solid was collected by filtration under N<sub>2</sub> using Schlenk glassware and dried in vacuo overnight. Yield: 0.08 g (~50%). Anal. Calcd for FeC<sub>20</sub>H<sub>22</sub>N<sub>6</sub>O<sub>6</sub>·0.75H<sub>2</sub>O: C, 46.75; H, 5.00; N, 16.36; Fe, 10.87. Found: C, 46.84; H, 4.40; N, 16.26; Fe, 10.42.

**Physical Measurements.** Magnetic susceptibility measurements were performed in the solid state by the Faraday technique using equipment previously described.<sup>26</sup> Solution susceptibilities were obtained by the Evans method<sup>27,28</sup> on a Varian EM-390 NMR spectrometer with Me<sub>4</sub>Si as the internal reference compound. Pascals' constants were used to correct for ligand diamagnetism: (5-NO<sub>2</sub>-Sal)<sub>2</sub>trien, -200 × 10<sup>-6</sup> cgsu.

Mössbauer spectra were obtained by using a previously described spectrometer<sup>8</sup> and computer fitted by the program of Chrissman and Tumolillo.<sup>29</sup> Sodium nitroprusside (SNP) was used as the reference compound, and the temperature was monitored by a copper vs. constantan thermocouple imbedded in the sample. Computer generated plots of the Mössbauer spectrum were obtained by using a Calcomp plotting program.

Solution conductivity measurements were measured by using a Model 31 YSI conductivity bridge. Chemical analyses were obtained commercially.

**Electrochemistry.** Polarographic measurements were made by using an EG & G Princeton Applied Research (PAR) Model 174 polarographic analyzer, utilizing the three-electrode system with a dropping mercury electrode (DME), a platinum wire counterelectrode, and a commercial saturated calomel reference electrode (SCE). An Omnigraphic 2000 recorder was used to record the current-voltage output. Cyclic voltammetry measurements were made by using either the PAR Model 174 with X-Y recorder or a PAR Model 175 universal programmer with a PAR Model 173 potentiostat and X-Y recorder or a Tektronix 5111 storage oscilloscope. A three-electrode configuration was used with platinum working and counterelectrodes and either a saturated calomel or commercial saturated lithium calomel electrode (SLCE) as the reference electrode. Sweep rates were varied between 0.02 and 2.0 V/s. For all the electrochemical experiments the reference electrode was separated from the solution by means of a fritted bridge filled with solvent and supporting electrolyte. The solution was changed periodically to prevent aqueous contamination of the solution from the reference electrode. Deaeration of all solutions was accomplished by passing a constant stream of high-purity nitrogen through the solution for 10 min and maintaining a blanket of nitrogen over the solution while making the measurements. The nitrogen was saturated with solvent prior to entering the cell. Controlled potential coulometry was performed by using a PAR Model 173 potentiostat equipped with a PAR Model 179 digital coulometer. The PAR Model 179's digital display indicated the accumulated coulombs. The current-time curve

- (10) R. M. Golding and K. Tettonen, *Aust. J. Chem.*, **27**, 2083 (1974).
- (11) R. H. Petty, E. V. Dose, M. F. Tweedle, and L. J. Wilson, *Inorg. Chem.*, **17**, 1064 (1978).
- (12) E. V. Dose, M. A. Hoselton, N. Sutin, M. F. Tweedle, and L. J. Wilson, *J. Am. Chem. Soc.*, **100**, 1141 (1978).
- (13) R. A. Binstead, J. K. Beattie, E. V. Dose, M. F. Tweedle, and L. J. Wilson, *J. Am. Chem. Soc.*, **100**, 5609 (1978).
- (14) M. A. Hoselton, L. J. Wilson, and R. S. Drago, *J. Am. Chem. Soc.*, **97**, 1722 (1975).
- (15) M. A. Hoselton, R. A. Drago, L. J. Wilson, and N. Sutin, *J. Am. Chem. Soc.*, **98**, 6967 (1976).
- (16) L. J. Wilson, D. Georges, and M. A. Hoselton, *Inorg. Chem.*, **14**, 2968 (1975).
- (17) J. K. Beattie, N. Sutin, D. H. Turner, and G. W. Flynn, *J. Am. Chem. Soc.*, **95**, 2052 (1973).
- (18) J. K. Beattie and R. J. West, *J. Am. Chem. Soc.*, **96**, 1933 (1974).
- (19) J. K. Beattie, R. A. Binstead, and R. J. West, *J. Am. Chem. Soc.*, **100**, 3044 (1978).
- (20) M. Sharrock, E. Munch, P. G. Debrunner, V. Marshall, J. D. Lipscomb, and I. Gunsalus, *Biochemistry*, **12**, 258 (1973).
- (21) D. F. Wilson, P. L. Dutton, M. Erecinska, J. G. Lindsay, and N. Sato, *Acc. Chem. Res.*, **5**, 234 (1972).
- (22) E. V. Dose, M. F. Tweedle, L. J. Wilson, and N. Sutin, *J. Am. Chem. Soc.*, **99**, 3886 (1977).
- (23) R. Chant, A. R. Hendrickson, R. L. Martin, and N. M. Rhode, *Inorg. Chem.*, **14**, 1894 (1975).
- (24) Hiroshi Yasude, Kosaku Suga, and Shigiru Aoyagui, *J. Electroanal. Chem. Interfacial Electrochem.*, **86**, 259 (1975).
- (25) E. Sinn, G. Sim, E. V. Dose, M. F. Tweedle, and L. J. Wilson, *J. Am. Chem. Soc.*, **100**, 3375 (1978).

- (26) M. F. Tweedle and L. J. Wilson, *Rev. Sci. Instrum.*, **49**, 1001 (1978).
- (27) D. F. Evans, *J. Chem. Soc.*, 2037 (1959).
- (28) D. Ostfeld and I. A. Cohen, *J. Chem. Educ.*, **49**, 829 (1972).
- (29) B. L. Chrissman and T. A. Tumolillo, *Comput. Phys. Commun.*, **2**, 322 (1975).

was also recorded on an X-Y recorder. The coulometric cell consisted of two compartments separated by a fritted disk. Platinum gauze served as both the anode and cathode. Stirring was achieved by using a magnetic stirring bar and motor.

**Variable-Temperature Electrochemistry.** The electroreduction of each compound was investigated in butyronitrile between 220 and 320 K. Variable-temperature cyclic voltammetry was performed by using the PAR Model 173 and Model 175 with an Omnigraphic 2000 recorder. A jacketed Brinkman titration vessel was used as the cell with platinum wire working and counterelectrodes and a SLCE reference electrode. The outer jacket of the cell was insulated to prevent condensation, and the entire cell was placed in an insulated box. The cell was cooled by circulating cold nitrogen gas through the jacket, utilizing a Varian variable-temperature controller. The nitrogen was cooled by passing it through a heat exchanger that was immersed in a Dewar of liquid nitrogen. The reference electrode was maintained at room temperature throughout the experiments and was separated from the solution by two fritted bridges, each containing solvent and supporting electrolyte. The SLCE and inner bridge were removed from the cell during cooling. The temperature of the solution was recorded with a thermometer ( $\pm 1$  °C). Deaeration was accomplished as described above. *IR* compensation between the working and reference electrodes was accomplished by utilizing the positive feedback from the PAR Model 176 current follower or Model 179 digital coulometer. The cell was allowed to reach a constant temperature before each measurement was taken.

In a nonisothermal cell of the type described above the temperature dependence of the standard reduction-oxidation potential of the species of interest can be separated into three components.<sup>30</sup> One of these is due to the Soret effect in which there is thermal migration of species due to the temperature gradient within the cell. Strong electrolytes will concentrate in the cold region, causing a change in electrode potentials. These potential shifts are usually in the order of hundredths of a millivolt per degree.<sup>31</sup> Since the solution of interest was purged with nitrogen during temperature changes and the reference electrode/bridge unit was removed during temperature changes, any concentration of electroactive species should be minimal and any potential changes due to Soret effect can be neglected.

A second component which must be considered is the thermal liquid junction potential. For aqueous solutions, a saturated or 3.5 M KCl salt bridge is normally employed<sup>32</sup> and the junction potential is assumed to be zero. However, in nonaqueous media the contribution to thermal liquid junction potential is unclear. The solubility of KCl in *n*-PrCN prevents use of a 3.5 M solution as a salt bridge. With use of a concentrated KCl bridge, KClO<sub>4</sub> will precipitate at the bridge junction, thus introducing an uncompensated resistance and a corresponding potential change greater than that of the thermal liquid junction which we would want to correct. Thus, due to our experimental design there is probably some small but unknown contribution to thermal liquid junction potential in our systems. The third contribution to the potential is the thermocouple effect of the metallic electrode. In our experiments this was negligible. Over the temperature range utilized, the greatest thermocouple potential for a Pt electrode is  $\sim 4.5$   $\mu$ V.<sup>31</sup>

With use of the Gibbs-Helmholtz equation,<sup>33</sup> it can be shown that

$$\Delta S_{et} = nF(dE^\circ/dT)_p \quad (2)$$

where  $\Delta S_{et}$  is the electron-transfer entropy for the process  $Ox + ne^- \rightleftharpoons Red$ . For a reversible process, in which the diffusion coefficients of the oxidized and reduced species are equal, the polarographic half-wave potential,  $E_{1/2}$ , is a good estimate of the standard electrode potential,  $E^\circ$ . Verification that  $D_{Ox} \approx D_{Red}$  and that the temperature coefficient of the oxidized and reduced species were equal was obtained by a measurement of the anodic and cathodic peak currents. At all temperatures investigated  $i_{pa}/i_{pc}$  were equal to unity. Thus the approximation that  $dE_{1/2}/dT \approx dE^\circ/dT$  is valid, and  $\Delta S_{et}$  may be obtained directly from the temperature variation of  $E_{1/2}$ .

Half-wave potentials were measured as the average of the anodic and cathodic peaks,  $(E_{pa} + E_{pc})/2$ . The pilot ion method, using

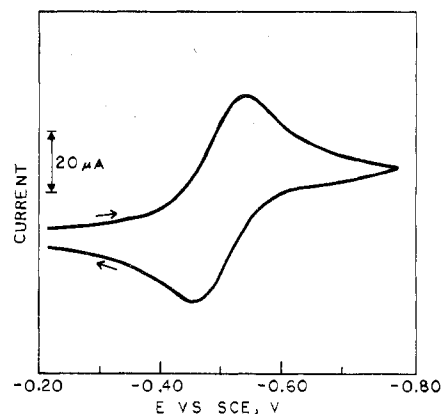


**Figure 2.** Cyclic voltammogram of  $9 \times 10^{-4}$  M  $[\text{Fe}(\text{Sal})_2\text{trien}]\text{PF}_6$  in  $\text{CH}_3\text{CN}$ , 0.1 M TBAP.

**Table I.** Half-Wave Potentials for Several  $[\text{Fe}(\text{X-Sal})_2\text{trien}]\text{PF}_6$  Compounds in  $\text{CH}_3\text{CN}$  at 293 K

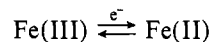
compd.	substituent, X	$2\sigma^a$	$E_{1/2}$ , V vs. SCE
1	5-NO <sub>2</sub>	1.56	-0.21
2	5-Br	0.54	-0.39
3	5-Cl	0.48	-0.40
4	H	0.00	-0.49
5	5-OCH <sub>3</sub>	-0.22	-0.53

<sup>a</sup>  $2\sigma$  is the substituent constant representing the sum of the inductive and/or polar effects of all substituents: J. March, "Advanced Organic Chemistry: Reactions, Mechanism, and Structure", McGraw-Hill, New York, 1977, p 253.  $2\sigma$  is used here since each iron complex contains two substituents.

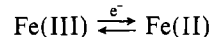
ferrocenium ion, was used to estimate liquid junction potential contributions to the measured half-wave potentials.<sup>34</sup>

## Results and Discussion

The electrochemical reduction of the  $[\text{Fe}^{\text{III}}(\text{X-Sal})_2\text{trien}]^+$  complexes is a one-electron transfer that is assigned as an



reaction. A typical cyclic voltammogram of  $[\text{Fe}^{\text{III}}(\text{Sal})_2\text{trien}]\text{PF}_6$  at a platinum electrode in  $\text{CH}_3\text{CN}$  is shown in Figure 2. In this solvent the half-wave potential was  $-0.49$  V vs. SCE. No other electrochemical processes were observed between  $+1.0$  and  $-1.5$  V vs. SCE. For each of the five complexes investigated, the



half-wave potential varied between  $-0.21$  and  $-0.53$  V vs. SCE depending on the solvent and/or substituent. Values in  $\text{CH}_3\text{CN}$  are listed in Table I as a function of the substituent.

In all cases, the increase of peak current and invariant peak potential with increasing sweep rates was characteristic of a diffusion-controlled reversible electron transfer.<sup>35</sup> For cyclic voltammetry,  $|E_p - E_{p/2}|$  was  $60 \pm 10$  mV. Polarographic wave analysis plots of  $E$  vs.  $\log(i/i_d - i)$  gave slopes of  $60 \pm 5$  mV, indicating a one-electron diffusion-controlled reduction. Half-wave potentials obtained by using platinum and Hg electrodes were almost identical. Controlled potential electrolysis also confirmed the presence of a one-electron diffusion-controlled reduction. Reduction in  $\text{CH}_3\text{CN}$  at controlled potential for the  $[\text{Fe}^{\text{III}}(\text{Sal})_2\text{trien}]^+$  parent compound required  $0.99 \pm 0.02$  electrons/mol to reduce the complex. During

(30) A. J. de Bethune, T. S. Licht and N. Swendeman, *J. Electrochem. Soc.*, **106**, 616 (1959).

(31) A. J. de Bethune, *J. Electrochem. Soc.*, **107**, 829 (1960).

(32) E. L. Yee, R. J. Cave, K. L. Guyer, P. D. Tyma, and M. J. Weaver, *J. Am. Chem. Soc.*, **101**, 1131 (1979).

(33) W. J. Moore, "Physical Chemistry", 4th ed., Prentice-Hall, Englewood Cliffs, N.J., 1972, p 85.

(34) J. B. Headridge, "Electrochemical Techniques for Inorganic Chemists", Academic Press, New York, 1969.

(35) R. S. Nicholson and I. Shain, *Anal. Chem.*, **36**, 706 (1964).

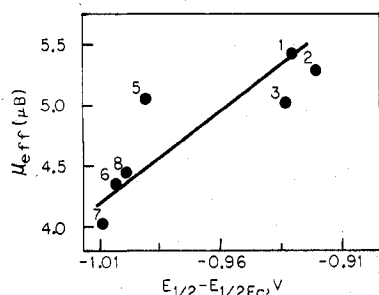


Figure 3.  $\mu_{\text{eff}}$  vs.  $(E_{1/2} - E_{1/2\text{Fc}})$  for  $[\text{Fe}(\text{Sal})_2\text{trien}]\text{PF}_6$ . Numbers correspond to solvents listed in Table II.

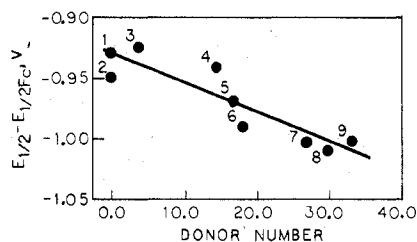


Figure 4.  $(E_{1/2} - E_{1/2\text{Fc}})$  vs. donor number for  $[\text{Fe}(\text{Sal})_2\text{trien}]\text{PF}_6$ . Numbers correspond to solvents listed in Table II.

reduction the color of the solution changed from tannish brown to light lavender. The solution was stable under  $\text{N}_2$ , and reoxidation could be accomplished with the abstraction of  $1.0 \pm 0.1$  electrons/mol as the solution returned to its original color. Under similar conditions the  $[\text{Fe}^{\text{II}}(5\text{-NO}_2\text{-Sal})_2\text{trien}]$  reduction product precipitated from solution and could thus be isolated as a solid (see Experimental Section).

**Solvent and Substituent Effect on Half-Wave Potentials.** As was shown earlier, the magnetic moment (and thus the  $^2\text{T}$  and  $^6\text{A}$  spin isomer concentrations) of the  $[\text{Fe}^{\text{III}}(\text{Sal})_2\text{trien}]^+$  cation is extremely solvent dependent.<sup>7</sup> For nine nonaqueous solvents varying from  $\text{CH}_2\text{Cl}_2$  to  $\text{Me}_2\text{SO}$ , the effective magnetic moment ( $\mu_{\text{eff}}$ ) at 307 K was found to range from  $5.41 \mu_{\text{B}}$  ( $\sim 20\%$   $^2\text{T}$ ,  $80\%$   $^6\text{A}$ ) to  $4.02 \mu_{\text{B}}$  ( $\sim 55\%$   $^2\text{T}$ ,  $45\%$   $^6\text{A}$ ). In this regard,  $\mu_{\text{eff}}$  also varies as the donor number<sup>36</sup> of the solvent gradually changes from 0.0 ( $\text{CH}_2\text{Cl}_2$ ) to 29.8 ( $\text{Me}_2\text{SO}$ ). Furthermore, it was shown that the source of this solvent dependency was related to strength of hydrogen bonding between the solvent and the amine protons of the  $\text{Sal}_2\text{trien}$  ligand (Figure 1), with stronger [solvent...HN] interactions shifting the  $^2\text{T}(\text{ls}) \rightleftharpoons ^6\text{A}(\text{hs})$  equilibrium to the left.<sup>7</sup> Figures 3 and 4 illustrate plots of  $\mu_{\text{eff}}$  vs.  $(E_{1/2} - E_{1/2\text{Fc}})$  and  $(E_{1/2} - E_{1/2\text{Fc}})$  vs. donor number for the  $[\text{Fe}^{\text{III}}\text{Sal}_2\text{trien}]^+$  cation in various solvents, where each of the potentials is reported as the difference between the measured  $\text{Fe}(\text{III})/\text{Fe}(\text{II})$  half-wave potential and the half-wave potential for the ferrocene/ferrocenium couple ( $E_{1/2} - E_{1/2\text{Fc}}$ , V). This approach corrects for any liquid junction contributions. As seen from the figures, the most positive  $\text{Fe}(\text{III})$  reduction potentials (easiest to reduce) are in  $\text{CH}_2\text{Cl}_2$  and  $\text{CH}_3\text{NO}_2$  while the most negative potentials are in  $\text{Me}_2\text{SO}$  and pyridine. These results demonstrate net stabilization of the  $\text{Fe}(\text{III})$  oxidation state as the solvent donor number increases to produce a greater concentration of the low-spin isomer. The half-wave potential for  $[\text{Fe}^{\text{III}}(\text{Sal})_2\text{trien}]^+$  in each of the solvents is given in Table II along with the donor numbers.

Within a given solvent the half-wave potential for the reduction of  $[\text{Fe}^{\text{III}}(\text{X-Sal})_2\text{trien}]^+$  also varies as a function of the substituent group, X. Electron-donating groups produced more difficult reductions while electron-withdrawing groups have the opposite effect. The nature of this effect has been

Table II. Half-Wave Potentials for  $[\text{Fe}(\text{Sal})_2\text{trien}]^+$  in Various Solvents

no.	solvent	donor no. <sup>a</sup>	$E_{1/2}$ , V	$E_{1/2} - E_{1/2\text{Fc}}$ , V
1	$\text{CH}_2\text{Cl}_2$	0.0	-0.45	-0.93
2	1,2-dichloroethane	0.0	-0.46	-0.95
3	$\text{CH}_3\text{NO}_2$	2.7	-0.52	-0.92
4	$\text{CH}_3\text{CN}$	14.1	-0.49	-0.94
5	<i>n</i> -PrCN	16.6	-0.48	-0.97
6	acetone	17.0	-0.43	-0.99
7	DMF	26.6	-0.52	-1.00
8	$\text{Me}_2\text{SO}$	29.8	-0.53	-1.01
9	py	33.1	-0.45	-1.00

<sup>a</sup> T. Sawyer and J. L. Roberts, Jr., "Experimental Electrochemistry for Chemists", Wiley, New York, 1974, p 174.

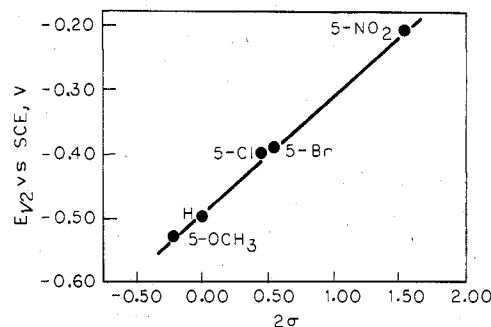


Figure 5.  $E_{1/2}$  vs.  $2\sigma$  for the  $[\text{Fe}^{\text{III}}(\text{X-Sal})_2\text{trien}]^+$  complexes.

examined by using the linear free-energy relationship of eq 3<sup>37</sup> where  $\sigma$  is the substituent constant representing the sum

$$\Delta E_{1/2} = 2\sigma\rho \quad (3)$$

of the inductive and/or polar effects of all substituents and  $\rho$ , the reaction constant, in volts, measures the sensitivity of the electron-transfer reaction to the effects of the substituent. In this work,  $2\sigma$  is utilized since there are two substituent groups per iron complex, the effect of which should be reflected in a plot of  $E_{1/2}$  vs.  $2\sigma$ . Such a plot is shown in Figure 5 for five of the compounds investigated in  $\text{CH}_3\text{CN}$  at 293 K. The electron-releasing  $5\text{-OCH}_3$  group makes the metal center more electron rich, thus producing a more difficult reduction process than for the unsubstituted parent compound, while the opposite is true for the electron-withdrawing  $5\text{-Cl}$ ,  $5\text{-Br}$ , and  $5\text{-NO}_2$  groups. Similar results were obtained in *n*-PrCN. The calculated reaction constant is 180 mV in  $\text{CH}_3\text{CN}$ . Of special interest in the plot is the fact that a linear relationship between  $E_{1/2}$  and  $2\sigma$  is observed despite the gradual change in the  $\text{Fe}(\text{III})$  spin state populations from mainly high spin ( $5\text{-OCH}_3$ ) to mainly low spin ( $5\text{-NO}_2$ ). This would imply that a similar reduction mechanism is operative for each member of the series and that the rate-determining step in the reduction mechanism is independent of the absolute high- or low-spin isomer populations. Similar linear relationships of  $E_{1/2}$  vs.  $2\sigma$  were obtained at temperatures between 220 and 300 K. It is significant to note that in Figures 3 and 4 a decrease in  $\mu_{\text{eff}}$  is associated with a more difficult reduction, while in Figure 5 compounds with reduced  $\mu_{\text{eff}}$  are more easily reduced. This would imply that when both solvent and substituent effects are considered simultaneously, a simple relationship does not exist between magnetic moment and half-wave potentials.

**Variable-Temperature Electrochemistry.** The electrochemical reduction of each compound in Table I was investigated as a function of temperature between 220 and 320 K. Plots were constructed of  $E_{1/2}$  vs.  $T$ , and from the slope of the line

(36) D. T. Sawyer and J. L. Roberts, Jr., "Experimental Electrochemistry for Chemists", Wiley, New York, 1974, p 174.

(37) P. Zuman, "Substituent Effects in Organic Polarography", Plenum Press, New York, 1967, p 31.

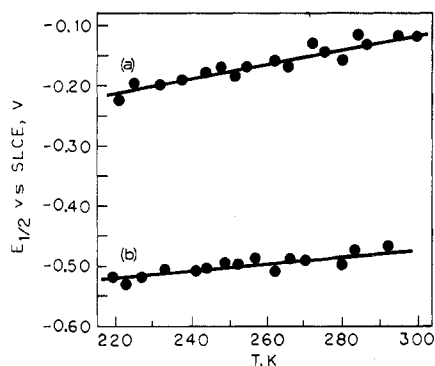


**Figure 6.** Temperature dependence of half-wave potential in *n*-PrCN, 0.1 M TBAP: (a)  $[\text{Fe}(5\text{-NO}_2\text{-Sal})_2\text{trien}]\text{PF}_6$ ,  $(\Delta E_{1/2}/\Delta T)_p = 1.18$  mV/K; (b)  $[\text{Fe}(5\text{-OCH}_3\text{-Sal})_2\text{trien}]\text{PF}_6$ ,  $(\Delta E_{1/2}/\Delta T)_p = 0.72$  mV/K.

**Table III.** Entropic Parameters for the Electroreductions and for the  ${}^2T \rightleftharpoons {}^6A$  Spin Crossovers of the  $[\text{Fe}^{\text{III}}(\text{X-Sal})_2\text{trien}]^+$  Cations

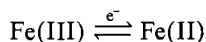
substituent	$\mu_{\text{eff}}$ (307 K) <sup>a</sup>	$(\Delta E_{1/2}/\Delta T)_p$ , <sup>b</sup> mV K <sup>-1</sup>	entropy change, eu	
			electron transfer, <sup>b,c</sup> $\Delta S_{\text{et}}$	spin crossover, <sup>a</sup> $\Delta S_{\text{sc}}$
5-OCH <sub>3</sub>	5.59 (85% hs)	0.72	16.6	16.7
H	5.05 (68% hs)	0.84	19.4	13.6
3-NO <sub>2</sub>	4.40 (49% hs)	0.91	21.0	12.5
5-NO <sub>2</sub>	3.15 (19% hs)	1.18	27.2	16.3

<sup>a</sup> Taken from ref 7. Measurements were made in acetone.

<sup>b</sup>  $[\text{Fe}^{\text{III}}(\text{X-Sal})_2\text{trien}]^+ + e^- \rightleftharpoons [\text{Fe}^{\text{II}}(\text{X-Sal})_2\text{trien}]$ . Measurements were made in *n*-PrCN containing 0.1 M TBAP as supporting electrolyte. <sup>c</sup> Calculated from eq 2 by using the approximation  $E_{1/2} \approx E^\circ$ . The uncertainty in the measured values are  $\pm 0.5$  eu.

the entropy of electron transfer,  $\Delta S_{\text{et}}$ , was calculated by utilizing eq 2. An example of the temperature dependence on  $E_{1/2}$  for reduction of the mainly low-spin 5-NO<sub>2</sub> and mainly high-spin 5-OCH<sub>3</sub> derivatives, in *n*-PrCN, is shown in Figure 6. The slopes  $(\Delta E_{1/2}/\Delta T)_p$ , for the 5-NO<sub>2</sub> and 5-OCH<sub>3</sub> species are 1.18 and 0.72 mV K<sup>-1</sup>, respectively, as determined by least-squares fitting of the data. These values correspond to electron-transfer entropies of 27.2 and 16.6 eu, respectively. Similar linear plots were obtained for each of the complexes investigated, and  $\Delta S_{\text{et}}$  was found to vary between the two extremes of 27.2 and 16.6 eu, as shown in Table III. These  $\Delta S_{\text{et}}$  values may be associated with changes in solvation entropies, changes in coordination geometry or number for the Fe(III) reactants and Fe(II) products, or changes in the spin states of the oxidized or reduced iron complexes. For the present  $[\text{Fe}(\text{X-Sal})_2\text{trien}]^+$  complexes, the Fe(III) and Fe(II) species are undoubtedly both six-coordinate, leaving the observed electron-transfer entropy changes due mainly to either solvation or spin-state-change effects. Furthermore, it is known from independent magnetic susceptibility measurements that the entropy change associated solely with the  ${}^2T \rightleftharpoons {}^6A$  spin-crossover processes ( $\Delta S_{\text{sc}}$ ) for the Fe(III) complexes varies between 12.5 and 16.7 eu (averaging 15.3 eu).<sup>7</sup> These values are also reproduced in Table III for each of the complexes studied.

When first initiated, it was hoped that this study might establish a relationship between the reversible Fe(III)/Fe(II) half-wave potentials (or  $\Delta S_{\text{et}}$ ) and the equilibrium constants or entropy changes ( $\Delta S_{\text{sc}}$ ) for the  ${}^2T \rightleftharpoons {}^6A$  spin crossovers. As illustrated by Figure 7, such a relationship does apparently exist between the % Fe(III)<sub>hs</sub> and  $\Delta S_{\text{et}}$  for these



reduction processes. From Table III it can be seen that  $\Delta S_{\text{sc}}$

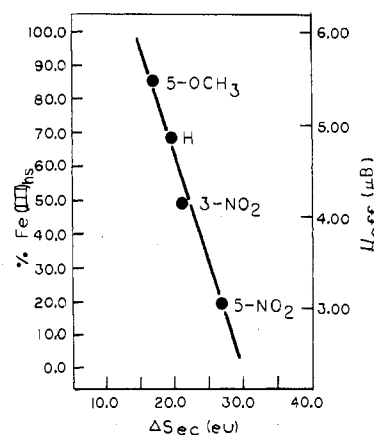


**Figure 7.** Percent high spin of Fe(III) vs. electron-transfer entropy for the  $[\text{Fe}(\text{X-Sal})_2\text{trien}]^+$  compounds. Spin-state data are from Table III.

is almost constant while  $\Delta S_{\text{et}}$  shows a considerable dependence on the high- and low-spin isomer populations, with a nearly linear relationship existing between % Fe(III)<sub>hs</sub> and the measured  $\Delta S_{\text{et}}$ . Moreover, examination of Figure 7 and Table III also reveals two other interesting features. First,  $\Delta S_{\text{et}}$  becomes larger as the low-spin population increases, and, second, extrapolation of  $\Delta S_{\text{et}}$  to 100% hs and 0% hs yields estimated values of 16 eu for reduction of the totally high-spin Fe(III) and 30 eu for reduction of the totally low-spin form. The difference between these two extremes yields  $\Delta S_{\text{sc}} = 14$  eu for the  ${}^2T \rightleftharpoons {}^6A$  spin crossover of the  $[\text{Fe}(\text{X-Sal})_2\text{trien}]^+$  system, and, within experimental error, this is the same value as determined by variable-temperature magnetic susceptibility measurements.<sup>7</sup>

**Electron-Transfer Mechanism.** The spin-equilibrium process for the  $[\text{Fe}^{\text{III}}(\text{Sal})_2\text{trien}]^+$  complexes manifests itself in a variation of the Fe-(donor atom) bond distances, with the low-spin form having bond distances that average 0.13 Å shorter than in the high-spin configuration.<sup>25</sup> In solution, this implies a solvation sphere that is more "ordered" for the low-spin form, and, thus, a positive  $\Delta S_{\text{sc}}$  contribution from solvation effects is to be expected for these  $l_s \rightarrow h_s$  processes. Furthermore, a small positive contribution to  $\Delta S_{\text{sc}}$  (ranging up to 2.18 eu)<sup>8</sup> for the change in spin degeneracy is also possible for these  $l_s \rightarrow h_s$  spin crossover processes. Thus, for a closely related series of compounds in a given solvent,  $\Delta S_{\text{sc}}$  is expected to be fairly constant, as is the case shown in Table III.

Upon electrochemical reduction of an  $[\text{Fe}^{\text{III}}(\text{X-Sal})_2\text{trien}]^+$  cation to produce the neutrally charged  $[\text{Fe}^{\text{II}}(\text{X-Sal})_2\text{trien}]$  species, the ligand field strength should be diminished due to charge reduction on the metal and the Fe(II) reduction products might, therefore, be expected to be high spin. The  $[\text{Fe}^{\text{II}}(5\text{-NO}_2\text{-Sal})_2\text{trien}]$  complex was isolated and characterized to verify this fact (see Experimental Section). The 5-NO<sub>2</sub> derivative was singled out for examination, because its Fe(III) analogue is the most low-spin member of the Fe(III) series, in solution, and, therefore, it seems reasonable that a high-spin  $[\text{Fe}^{\text{II}}(5\text{-NO}_2\text{-Sal})_2\text{trien}]$  species would imply high-spin ground states for the other Fe(II) derivatives as well. As expected, the  $[\text{Fe}^{\text{II}}(5\text{-NO}_2\text{-Sal})_2\text{trien}]$  compound was found to exhibit a magnetic moment (4.90  $\mu_B$  at 300 K and 100 K) and a Mössbauer spectrum ( $\delta = 1.45$  mm s<sup>-1</sup> (SNP),  $\Delta E_Q = 2.91$  mm s<sup>-1</sup> at 105 K) consistent with a high-spin  $S = 2$  ground state in the solid state.<sup>38</sup> The Mössbauer spectrum is shown in Figure 8. In CH<sub>3</sub>CN at 10<sup>-4</sup> M the compound

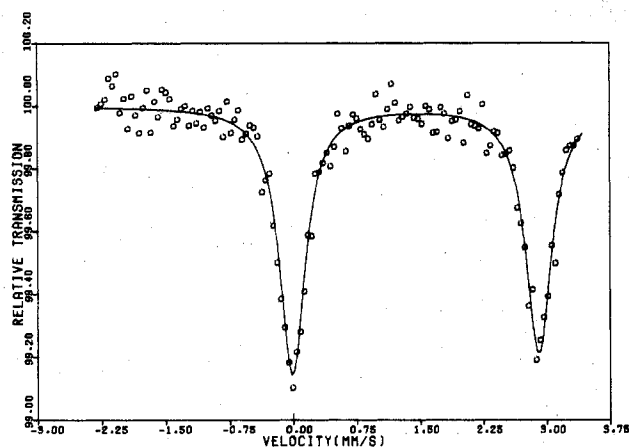
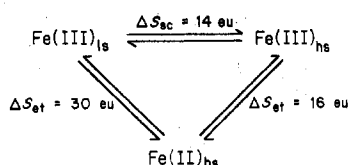


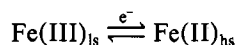
Figure 8. Mössbauer spectrum of  $[\text{Fe}^{\text{II}}(5\text{-NO}_2\text{-Sal})_2\text{trien}]$  at 105 K.

#### Scheme I



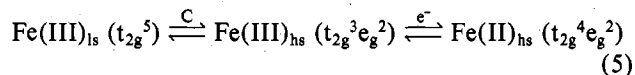
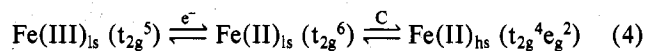
is a nonelectrolyte with  $\Lambda = 22 \Omega^{-1} \text{ cm}^{-1} \text{ M}^{-1}$ , but solubility limitations precluded an accurate measurement of  $\mu_{\text{eff}}$  by the Evans method in  $\text{CH}_3\text{CN}$  or  $n\text{-PrCN}$  (the primary electrochemical media). However, in  $\text{Me}_2\text{SO}-d_6$ ,  $\mu_{\text{eff}}(300 \text{ K}) = 4.2 \mu_{\text{B}}$  which indicates essentially high-spin Fe(II) in the solvent most likely to produce the strongest ligand field for the  $(5\text{-NO}_2\text{-Sal})_2\text{trien}$  ligand via  $[\text{solvent} \cdots \text{HN}]$  hydrogen bonding.<sup>7</sup> Thus, it is relatively certain that all the  $[\text{Fe}^{\text{II}}(\text{X-Sal})_2\text{trien}]$  reduction products are fully high spin in the solvents used for the electrochemical studies.

Having established the spin state of the Fe(II) reduction products, we propose the overall electron-transfer mechanism shown in Scheme I as being consistent with the electrochemical data. In the scheme, the Fe(III) complexes exist in equilibrium as either low-spin or high-spin species, with both forms being reduced to  $\text{Fe(II)}_{\text{hs}}$ . Reduction of  $\text{Fe(III)}_{\text{ls}}$  yields  $\Delta S_{\text{et}} = 30 \text{ eu}$ , whereas the reduction of  $\text{Fe(III)}_{\text{hs}}$  is associated with  $\Delta S_{\text{et}} = 16 \text{ eu}$ . Mixtures of high- and low-spin populations will be related to the percentage of each form present, as shown in Table III and Figure 7. With the assumption that the ultimate reduction products are  $\text{Fe(II)}_{\text{hs}}$ , there is still the problem of determining the actual electron-transfer mechanism for the



couple. I.e., does spin crossover occur before or after electron transfer?

Two possible pathways are represented by reactions 4 and 5. Reaction 4 involves a chemical reaction (spin crossover)



of Fe(II) following electron transfer (EC mechanism), whereas reaction 5 involves an internal chemical reaction of Fe(III) preceding electron transfer (CE mechanism). Both reactions 4 and 5 involve the same ultimate reactants and products, with electron transfer occurring only between Fe(III) and Fe(II) of like spin state, e.g.



Of course, this analysis assumes that electron transfer between redox species of differing spin multiplicities is spin forbidden or, at least, spin restricted, thereby permitting us to exclude the  $\text{Fe(III)}_{\text{ls}}/\text{Fe(II)}_{\text{hs}}$  and  $\text{Fe(III)}_{\text{hs}}/\text{Fe(II)}_{\text{ls}}$  couples as possibilities. However, the possibility cannot be ruled out that both reactions 4 and 5 are operative with one perhaps predominant over the other.

In many instances, differentiation between EC (reaction 4) and CE (reaction 5) mechanisms can be accomplished electrochemically by the use of variable-scan-rate studies and the monitoring of peak current and peak potentials as a function of potential sweep.<sup>39</sup> However, dynamics of  ${}^2\text{T} \rightleftharpoons {}^6\text{A}$  spin crossover for these  $[\text{Fe}^{\text{II}}(\text{X-Sal})_2\text{trien}]^+$  complexes are characterized by first-order rate constants of  $10^7\text{--}10^8 \text{ s}^{-1}$ , making these spin-transition processes too fast to observe on the cyclic voltammetry time scale. Thus, the only remaining way to possibly differentiate between reactions 4 and 5 appears to be by heterogeneous electron-transfer kinetics, since precedent in the literature indicates that the rates of heterogeneous electron transfer should be in the order  $\text{Fe(III)}_{\text{ls}}/\text{Fe(II)}_{\text{ls}} > \text{Fe(III)}_{\text{hs}}/\text{Fe(II)}_{\text{hs}}$ . Such studies are presently in progress on these and other variable-spin systems.

**Acknowledgment.** We gratefully acknowledge the Robert A. Welch Foundation [Grants E-680 (K.M.K.) and C-627 (L.J.W.)], the National Institutes of Health [Grant GM 25172-02 (K.M.K.)], the National Science Foundation [Grant CHE 77-14594 (L.J.W.)], and the donors of the Petroleum Research Fund, administered by the American Chemical Society (L.J.W.), for support of this work. In addition, we wish to thank Ms. Sharon Clarke for preliminary electrochemical experiments and Mr. Larry Bottomley for synthesizing several of the compounds.

**Registry No.**  $[\text{Fe}(5\text{-NO}_2\text{-Sal})_2\text{trien}]\text{PF}_6$ , 74111-30-1;  $[\text{Fe}(5\text{-Br-Sal})_2\text{trien}]\text{PF}_6$ , 74050-80-9;  $[\text{Fe}(5\text{-Cl-Sal})_2\text{trien}]\text{PF}_6$ , 74050-82-1;  $[\text{Fe}(\text{Sal})_2\text{trien}]\text{PF}_6$ , 74050-83-2;  $[\text{Fe}(5\text{-OCH}_3\text{-Sal})_2\text{trien}]\text{PF}_6$ , 74111-32-3;  $\text{Fe}(5\text{-NO}_2\text{-Sal})_2\text{trien}$ , 74050-84-3;  $\text{Fe}(5\text{-Br-Sal})_2\text{trien}$ , 74050-85-4;  $\text{Fe}(5\text{-Cl-Sal})_2\text{trien}$ , 74050-86-5;  $\text{Fe}(\text{Sal})_2\text{trien}$ , 74050-87-6;  $\text{Fe}(5\text{-OCH}_3\text{-Sal})_2\text{trien}$ , 74050-88-7;  $[\text{Fe}(3\text{-NO}_2\text{-Sal})_2\text{trien}]^+$ , 74111-33-4;  $\text{Fe}(3\text{-NO}_2\text{-Sal})_2\text{trien}$ , 74050-89-8.

(39) R. S. Nicholson and I. Shain, *Anal. Chem.*, **36**, 706 (1964).